

Cilostazol Protects Endothelial Cells Against Lipopolysaccharide-Induced Apoptosis Through ERK1/2- and P38 MAPK-Dependent Pathways

Jong-Hoon Lim¹, Jae-Suk Woo² and Yung-Woo Shin¹

Departments of ¹Internal Medicine and ²Physiology, Pusan National University College of Medicine, Busan, Korea

Background/Aims: We examined the effects of cilostazol on mitogen-activated protein kinase (MAPK) activity and its relationship with cilostazol-mediated protection against apoptosis in lipopolysaccharide (LPS)-treated endothelial cells.

Methods: Human umbilical vein endothelial cells (HUVECs) were exposed to LPS and cilostazol with and without specific inhibitors of MAPKs; changes in MAPK activity in association with cell viability and apoptotic signaling were investigated.

Results: Cilostazol protected HUVECs against LPS-induced apoptosis by suppressing the mitochondrial permeability transition, cytosolic release of cytochrome *c*, and subsequent activation of caspases, stimulating extracellular signal-regulated kinase (ERK1/2) and p38 MAPK signaling, and increasing phosphorylated cAMP-responsive element-binding protein (CREB) and Bcl-2 expression, while suppressing Bax expression. These cilostazol-mediated cellular events were effectively blocked by MAPK/ERK kinase (MEK1/2) and p38 MAPK inhibitors.

Conclusions: Cilostazol protects HUVECs against LPS-induced apoptosis by suppressing mitochondria-dependent apoptotic signaling. Activation of ERK1/2 and p38 MAPKs, and subsequent stimulation of CREB phosphorylation and Bcl-2 expression, may be responsible for the cellular signaling mechanism of cilostazol-mediated protection. (*Korean J Intern Med* 2009;24:113-122)

Keywords: Cilostazol; Protection, Endothelial Cells; Apoptosis; Extracellular signal-Regulated MAP Kinases 1/2; p38 Mitogen-Activated Protein Kinase

INTRODUCTION

Cilostazol, a quinolinone derivative synthesized by Otsuka Pharmaceutical Co. (Tokushima, Japan), is a specific inhibitor of phosphodiesterase III. Its principal actions are associated with its ability to elevate intracellular adenosine 3',5'-cyclic monophosphate (cAMP) levels, and include the inhibition of platelet aggregation [1,2] and enhancement of the microcirculation via vasodilation [3]. The drug has been approved by the US Food and Drug Administration for use in treating

intermittent claudication, which also involves its action in inhibiting the breakdown of cellular cAMP [4].

Damage to large vessel and microvascular endothelium is an important event in many forms of impaired organ function under a variety of pathological tissue conditions, including ischemia [5-7], shock [8], and sepsis [9]. Recently, several lines of evidence have suggested that cilostazol provides beneficial effects in protecting cells from injuries of diverse causes. Kim et al [10] reported a protective effect of cilostazol against lipopolysaccharide (LPS)-induced apoptosis in human umbilical vein

Received: June 2, 2008

Accepted: September 17, 2008

Correspondence to Jae-Suk Woo, MD

Department of Physiology, Pusan National University College of Medicine, 1ga-10 Ami-dong, Seo-gu, Busan 602-739, Korea
Tel: 82-51-510-8072, Fax: 82-51-510-8070, E-mail: jswoo@pusan.ac.kr

endothelial cells (HUVECs). In their study, they demonstrated a reversal by cilostazol of the LPS-induced decrease in Bcl-2 and increases in Bax proteins and cytochrome *c* release. Hong et al. [11] demonstrated the prevention of tumor necrosis factor- α -induced cell death in human neuroblastoma cells by cilostazol. An *in vivo* study in an animal model of middle cerebral artery occlusion and reperfusion also provided evidence for the protective effect of cilostazol against cerebral infarcts evoked via its anti-apoptotic actions. These reports provide consistent evidence that cilostazol can reduce apoptotic cell death by inhibiting the mitochondria-dependent apoptotic signaling pathway [12]. However, the precise site and mechanism of cilostazol-induced protection, apparently upstream of the mitochondrial phase, remain unknown.

Members of the mitogen-activated protein kinase (MAPK) family are important mediators of signal transduction pathways that serve to coordinate the cellular response to a variety of extracellular stimuli. Based on structural differences, the MAPK family has been classified into three major subfamilies: the extracellular signal-regulated kinase (ERK1/2), the c-Jun N-terminal kinase (JNK/SAPK), and the p38 MAPK [13] subfamilies. These kinases are activated by phosphorylation of both tyrosine and threonine residues catalyzed by specific upstream MAPKs. Activated MAPKs phosphorylate their specific substrates on serine and/or threonine residues, ultimately leading to activation of various transcription factors and control of a vast array of physiological processes, including cell survival and death [14].

In this study, we examined the effects of cilostazol on MAPK activity and its relationship with cilostazol-mediated protection against apoptosis in LPS-treated endothelial cells. HUVECs were exposed to LPS and cilostazol with or without specific inhibitors of MAPKs, and the changes in MAPK activity in association with cell viability and apoptotic signaling were determined.

METHODS

Chemicals

The cilostazol was a gift from Dr. Rhim (Department of Pharmacology, Pusan National University School of Medicine, Korea). Lipopolysaccharides were purchased from Sigma-Aldrich (St. Louis, MO, USA). Ac-DEVD-CHO, Z-IETD-FMC, Z-LEHD-FMK, Z-VAD-FMK, PD 98059, SB203580, SP600125, and U0126 were acquired

from Calbiochem (San Diego, CA, USA). TMRM, calcein/AM and DiOC₆(3) were obtained from Molecular Probes (Eugene, OR, USA). Antibodies to cytochrome *c*, Bcl-2, CREB, P-CREB, Bax, PERK1/2, P-p38, P-c-Jun and α -actin were purchased from Cell Signaling Technology (Beverly, MA, USA).

Cell culture

HUVECs, an endothelial cell line derived from the vein of a normal human umbilical cord (CRL-2480; American Type Culture Collection, Rockville, MD, USA), were cultured in Ham's F-12K medium supplemented with 10% heat-inactivated fetal bovine serum, 0.1 mg/mL heparin sodium, 0.03-0.05 mg/mL endothelial cell growth supplement, 100 U/mL penicillin, and 100 g/mL streptomycin. Cells were grown to confluence at 37°C in a humidified 95% air/5% CO₂ atmosphere in culture dishes coated with 0.1% gelatin. When the cultures reached confluence, subcultures were prepared, using a 0.02% ethylenediaminetetraacetic acid (EDTA)/0.05% trypsin solution.

Analysis of apoptosis

To detect apoptotic cells, the terminal transferase uridyl nick end labeling (TUNEL) assay was performed using the ApopTag Peroxidase In Situ Apoptosis Detection Kit (Intergen, Purchase, NY, USA). Briefly, cells cultured on coverglasses were exposed to experimental protocols and fixed in 1% paraformaldehyde for 10 min. The fixed cells were incubated with digoxigenin-conjugated dUTP in a TdT-catalyzed reaction for 60 min at 37°C and were then immersed in stop/wash buffer for 10 min at room temperature. The cells were then incubated with anti-digoxigenin antibody conjugated with peroxidase for 30 min. The DNA fragments were stained using 3,3'-diaminobenzidine (DAB) as a substrate.

Western blot analysis and immunoblotting

Cells were harvested and disrupted in lysis buffer (1% Triton X-100, 1 mM ethylene glycol tetraacetic acid (EGTA), 1 mM EDTA, 20 mM Tris-HCl (pH 7.4)). Cell debris was removed by centrifugation (10,000 g, 10 min, 4°C). The resulting supernatants were separated by 15% SDS-PAGE under denaturing, reducing conditions and transferred to nitrocellulose membranes. The membranes were blocked with 5% nonfat dried milk at room temperature for 30 min and incubated with antibodies against phosphorylated ERK1/2 (P-ERK), and phosphorylated

p38 (P-p38), cytochrome c, CREB and phosphorylated CREB (PCREB), Bcl-2, and Bax. The membranes were washed and incubated with the respective secondary antibodies. The signals were visualized using an enhanced chemiluminescence system (Amersham, Buckinghamshire, UK).

Assay of JNK activity

JNK activity was assayed with a nonradioactive assay kit, following the manufacturer's protocol (Cell Signaling Technology). Briefly, JNK protein was precipitated from the cell lysate by a c-Jun fusion protein bound to glutathione-Sepharose beads. C-Jun contains a high-affinity binding site for JNK, particularly the NH₂-terminal region to the two phosphorylation sites, Ser-63 and Ser73. After selectively pulling down JNK using the c-Jun fusion protein beads, the beads were extensively washed, and the kinase reaction was carried out in the presence of cold ATP in a final volume of 20 μ L. The reaction was stopped with 25 μ L of 2 \times Laemmli buffer and loaded onto a 15% polyacrylamide gel. Protein was transferred to nitrocellulose by electroblotting, and c-Jun phosphorylation was selectively assessed using a phospho-c-Jun antibody. This antibody specifically measures JNK-induced phosphorylation of c-Jun at Ser-63, a site important for c-Jun-dependent transcriptional activity [15].

Determination of caspase activity

A quantitative enzymatic activity assay was carried out using a colorimetric assay kit according to manufacturer's protocol (R&D Systems, Minneapolis, MN, USA). Cells were harvested, washed with ice-cold phosphate-buffered saline (PBS), lysed, centrifuged, and analyzed for total protein by the Bradford assay. Reaction buffer (25 μ L) containing 10 mM dithiothreitol and 6 μ L fluorogenic caspase-specific substrate (DEVD-pNA for caspase 3, Ac-IETD-pNA for caspase 8, and Ac-LEHD-pNA for caspase 9) was added to each sample, and the samples were incubated at 37°C for 2 hour. Protease activity was determined by measuring the relative fluorescence intensity at 505 nm after excitation at 400 nm using a luminescence spectrometer (LS50B; Perkin Elmer, Buckinghamshire, UK). Results are shown as fold increases in activity relative to untreated control cells.

Measurement of mitochondrial membrane potential

The mitochondrial transmembrane potential was

measured using DiOC₆(3), a fluorochrome that is incorporated into cells depending on the mitochondrial membrane potential [16]. Reduced DiOC₆(3) staining indicates disruption of the mitochondrial inner trans-membrane potential. Cells were stained with DiOC₆(3) at a final concentration of 50nM for 20min at 37°C in the dark. Cells were washed and resuspended in PBS. The fluorescence intensity was analyzed with a FACsort flow cytometer (Becton Dickinson, Laguna Hills, CA, USA).

Confocal microscopic analysis of mitochondrial permeability transition

To determine the changes in mitochondrial permeability and membrane potential, a double-staining method with fluorescent dyes, calcein-AM and tetramethylrhodamine methyl ester (TMRM), was used as described by Lemasters et al. [17] Intact mitochondria maintain an inside-negative membrane potential and accumulate the lipophilic cationic dye TMRM, with bright yellow fluorescence. As calcein is impermeable to the inner mitochondrial membrane, it does not enter the mitochondria. However, mitochondrial dysfunction caused by a mechanism referred to as the "mitochondrial permeability transition" (MPT) makes the mitochondria permeable to solutes and depolarizes the membrane potential. Thus, *injured* mitochondria lose TMRM and become permeable to and stained by calcein (green).

Statistical analyses

The data are expressed as means \pm SE. The significance of difference between two groups was evaluated by Student's *t*-test. Multiple group comparisons were performed using a one-way analysis of variance, followed by the Tukey's *post hoc* test. A *p* value <0.05 was deemed to be statistically significant.

RESULTS

LPS-induced apoptosis and protection by cilostazol

When HUVECs were assessed by TUNEL staining after 18 hours exposure to 0.1 μ g/mL LPS, apoptotic cells with nuclear condensation and fragmentation were observed (Fig. 1A). The extent of LPS-induced apoptosis was concentration-dependent in the range from 0.01 to 1 μ g/mL. At a concentration of 1 μ g/mL, 47.6 \pm 6.8% of the cells were counted as apoptotic (Fig. 1B). The results in

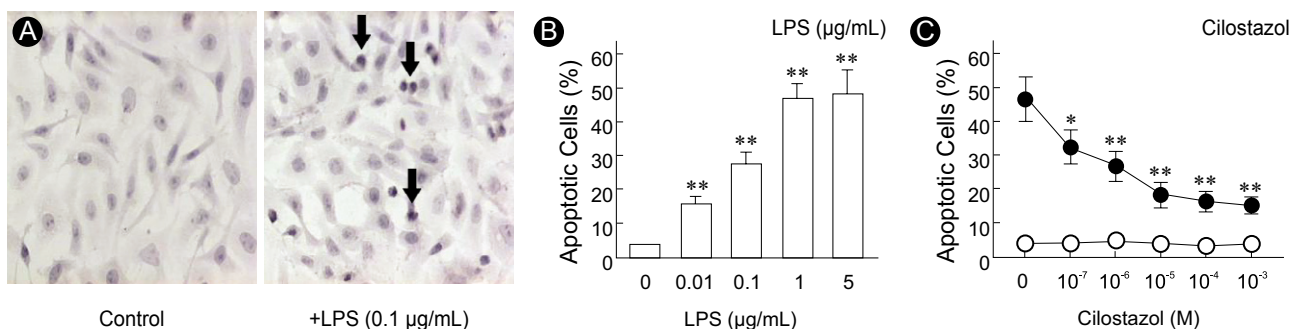


Figure 1. LPS-induced apoptosis and its protection by cilostazol. Cells were exposed to indicated concentrations of LPS in the presence or absence of cilostazol for 18 hours. Cells were pre-treated with cilostazol 15 min prior to the exposure to LPS. Apoptotic cells were detected by TUNEL assay. A. Representative micrographs of TUNEL-stained control and LPS-treated cells. Arrows indicate representative apoptotic cells. B. Concentration-dependent effect of LPS to induce apoptosis. C. Concentration-dependent protection by cilostazol against apoptosis in LPS-treated cells. Each point in B and C represents mean±S.E. of 4 experiments. **p*<0.05 and ***p*<0.01 vs. respective controls without drugs (LPS in B and cilostazol in C)

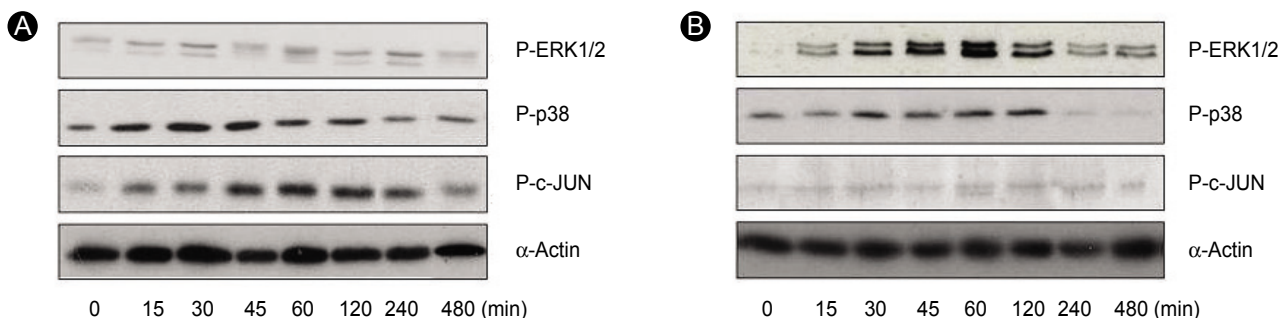


Figure 2. LPS- and cilostazol-induced activation of MAPKs. Cells were treated with 1 μg/mL LPS (A) or 10 μM cilostazol (B) for the indicated time periods, and the levels of phosphorylation for each MAPK subfamily were determined by Western blot analysis of cellular extracts.

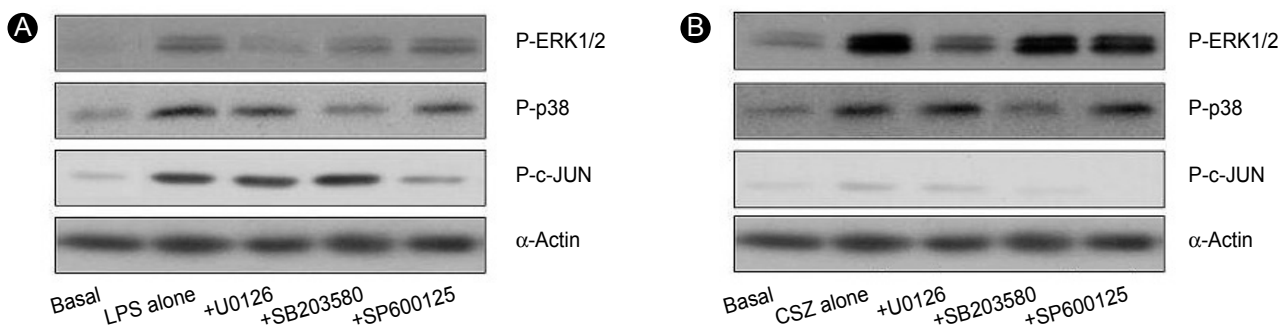


Figure 3. Effects of MAPK inhibitors on the LPS- and cilostazol-induced activation of MAPKs. Cells were treated with 1 μg/mL LPS (A) or 10 μM cilostazol (B) in the presence of different MAPK inhibitors (each 20 μM) for 45 min, and the phosphorylated levels of each MAPK subfamily were determined by Western blot analysis of cellular extracts.

Figure 1C show concentration-dependent protection by cilostazol against LPS-induced apoptosis. The concentration of cilostazol to reduce LPS-induced apoptosis by 50% was $1.1 \pm 24 \times 10^{-6}$ M. In the following experiments, when cells were treated with cilostazol, a 10 μM concentration was applied 15 min prior to exposure to LPS. At this concentration, cilostazol provided protection against LPS-induced apoptosis by $70.9 \pm 8.6\%$. Cilostazol alone

did not affect cell viability in the concentration range tested (10^{-7} to 10^{-3} M).

LPS- and cilostazol-induced activation of MAPKs

To evaluate the possible involvement of MAPKs in the LPS- and cilostazol-mediated changes in cell survival signaling, activation of MAPK subfamilies was estimated by measuring their phosphorylation levels. Cells were

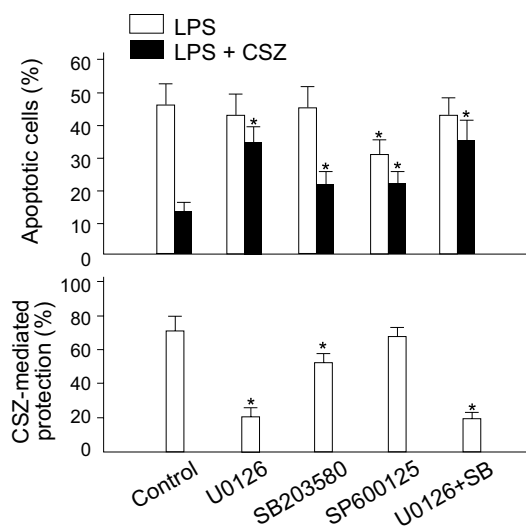


Figure 4. Effects of MAPK inhibitors on LPS-induced apoptosis and protection from it by cilostazol. Cells were treated with 1 $\mu\text{g}/\text{mL}$ LPS or 10 μM cilostazol in the presence of different MAPK inhibitors (each 20 μM) for 18 hours. Apoptotic cells were detected by the TUNEL assay. Each bar represents the mean \pm SE of five experiments. * $p < 0.01$ vs. control.

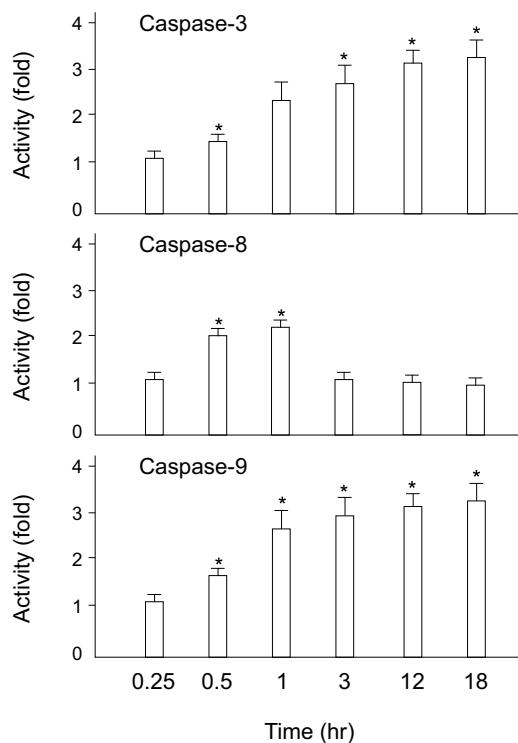


Figure 5. Effects of LPS on caspase activity. Cells were treated with 1 $\mu\text{g}/\text{mL}$ LPS for the indicated time periods and assayed for caspases 3, 8, and 9 activity. Each bar represents the mean \pm SE of five experiments. * $p < 0.01$ vs. respective control.

treated with 1 $\mu\text{g}/\text{mL}$ LPS or 10 μM cilostazol for the indicated time periods. Cells treated with LPS exhibited elevated phosphorylation levels of P-p38 and P-c-JUN.

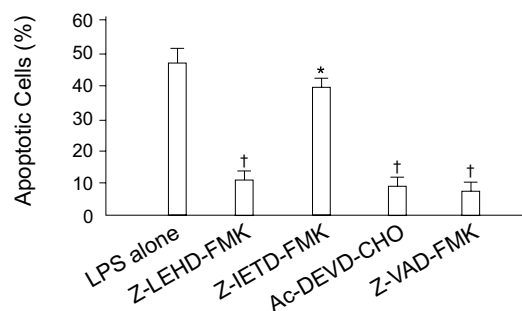


Figure 6. Effects of caspase inhibitors on LPS-induced apoptosis. Cells were treated with 1 $\mu\text{g}/\text{mL}$ LPS in the presence of different caspase inhibitors (each 20 μM) for 18 hours. Apoptotic cells were detected by the TUNEL assay. The number of apoptotic cells is represented as the percentile of total cell counts. Each bar represents the mean \pm SE of six experiments. * $p < 0.05$, † $p < 0.01$ vs. control.

Elevation of these phosphoprotein levels was apparent after 15 min of treatment and reached peak levels at 30 min for P-p38 and 60 min for P-c-JUN. LPS caused no significant change in the phosphorylation level of ERK1/2 (Fig. 2A). In contrast, cilostazol induced a marked increase in ERK1/2 phosphorylation levels. Elevation of P-ERK1/2 was detectable after 15 min of exposure to cilostazol and reached a peak at 60 min. Cilostazol also induced elevated phosphorylation levels in p38, although it did not affect JNK activity (Fig. 2B). Elevation of these phosphorylated proteins was selectively blocked by the MEK1/2 inhibitor U0126 [18], the p38 MAPK inhibitor SB203580 [19], and the JNK inhibitor SP600125 [20], indicating that LPS- or cilostazol-induced changes in these phosphorylated proteins was associated with selective activation of MAPKs (Fig. 3).

Effects of MAPK inhibitors on apoptosis

To examine whether activation of the MAPK pathway was involved in LPS-induced apoptosis and the protection by cilostazol, the effects of MAPK inhibitors were studied. In the absence of cilostazol, LPS-induced apoptosis was unaffected by U0126 or SB203580, suggesting that LPS evoked apoptosis through a mechanism independent of ERK1/2 or p38 MAPK. In contrast, U0126 significantly reduced the cilostazol-mediated protection against apoptosis in LPS-treated cells. SB203580 also reduced cilostazol-mediated protection (Fig. 4). These results, consistent with those in Figures 2 and 3, suggest that the signaling mechanism underlying the cilostazol-mediated protection against apoptosis in LPS-treated cells was associated with activation of the ERK1/2 and p38 MAPK pathways.

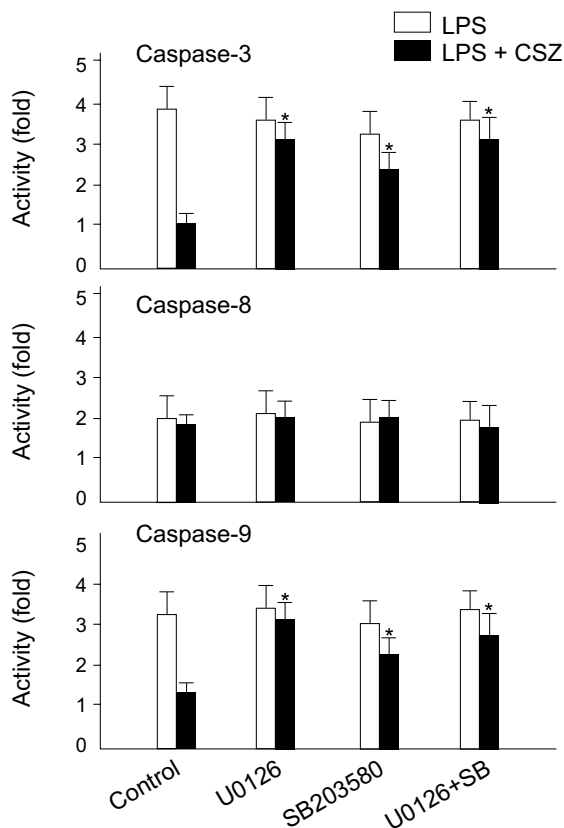


Figure 7. Effects of MAPK inhibitors on LPS- and cilostazol-induced changes in caspase activity. Cells were treated with 1 µg/mL LPS with and without 10 µM cilostazol in the presence of different MAPK inhibitors (each 20 µM) for 45 min, and assayed for caspases 3, 8, and 9 activities. Each bar represents the mean±SE of four experiments. * *p*<0.01 vs. control.

Role of caspases in LPS-induced apoptosis

Activation of caspase cascades is key for the execution phase of apoptosis. Caspase 9 is activated by cytochrome *c* released from mitochondria and is thus crucial for the execution of mitochondria-dependent apoptosis, whereas caspase 8 is activated largely through a mitochondria-independent mechanism [17]. Caspase 3, which is activated by the active form of caspase 8 or 9, is a protease that mediates apoptosis. To delineate the role of these caspases in the LPS-induced apoptosis, we investigated the activation pattern of these caspases in LPS-treated cells. Cells were treated with 1 µg/mL LPS for the indicated time periods and the lysate was incubated with a fluorogenic substrate, the Ac-LEHD-fmk motif, of the enzyme. LPS-induced activation of caspase 9 showed a time-dependent and sustained pattern. The activity reached a peak (3.1-fold increase) at 3 hour and remained elevated up to 18 hours. In contrast, caspase 8 was transiently activated by LPS, showing peak activity (1.9-fold increase) at 30 min, followed by a return to the control value at 3 hour. Activation of caspase 3 was similar to that of caspase 9 (Fig. 5).

To delineate the role of these caspases in LPS-induced apoptosis, the effects of caspase inhibitors were examined. Z-LEHD-FMK [21] and Ac-DEVD-CHO [22], specific inhibitors of caspases 9 and 3, respectively, and the broad-range caspase inhibitor, Z-VAD-FMK [23], all markedly prevented LPS-induced apoptosis. In contrast, the caspase 8 inhibitor Z-IETD-FMK [24] showed only

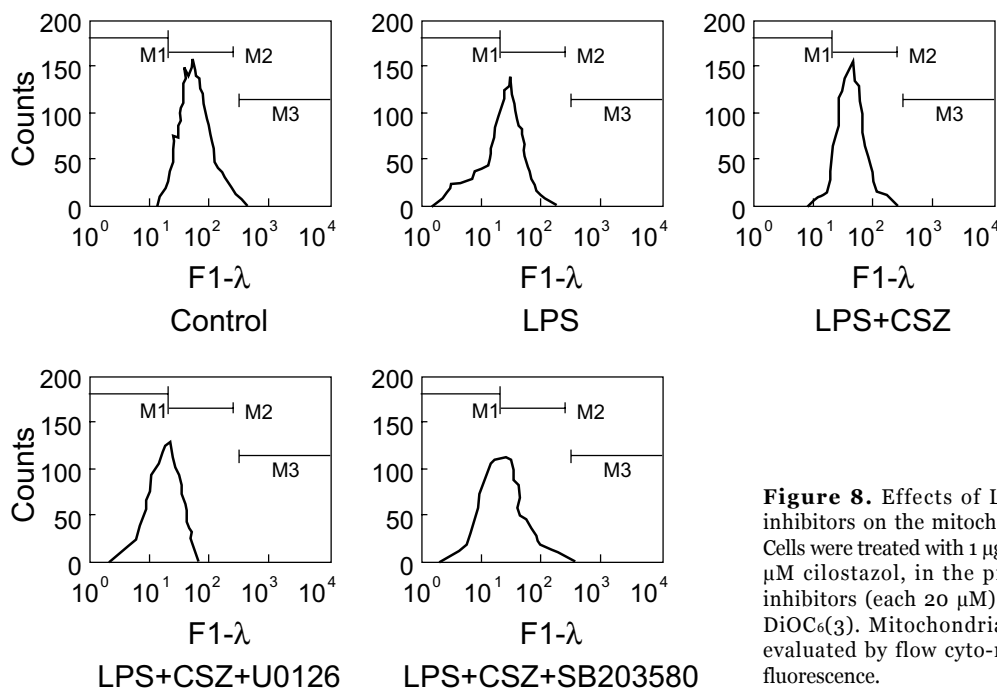


Figure 8. Effects of LPS, cilostazol, and MAPK inhibitors on the mitochondrial membrane potential. Cells were treated with 1 µg/mL LPS with and without 10 µM cilostazol, in the presence of different MAPK inhibitors (each 20 µM) for 6 hour and loaded with DiOC₆(3). Mitochondrial membrane potential was evaluated by flow cytometric analysis of DiOC₆(3) fluorescence.

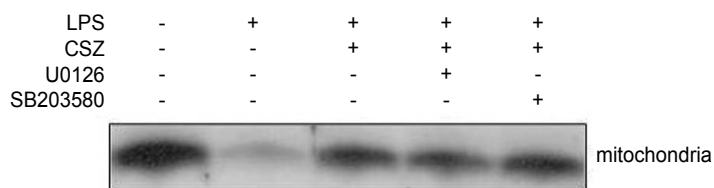


Figure 9. Effects of LPS, cilostazol, and MAPK inhibitors on the cytosolic release of cytochrome *c*. Cells were treated with 1 $\mu\text{g}/\text{mL}$ LPS with and without 10 μM cilostazol, in the presence of different MAPK inhibitors (each 20 μM) for 18 hours, and Western blot analysis was performed for cytochrome *c* in the mitochondrial and cytosolic fractions of cell extracts.

a minimal protective effect (Fig. 6). These results suggest that activation of caspase 9 through a mitochondria-dependent mechanism plays a key role in LPS-induced apoptosis in HUVECs.

Effects of MAPK inhibitors on caspase activity

To delineate the link between cilostazol-mediated activation of MAPKs and the inhibition of caspase activation, the effects of U0126 and SB203580 on caspase activity in LPS- and/or cilostazol-treated cells were examined. LPS transiently activated caspase 8 (Fig. 5). It was unaffected by U0126 and SB203580 in the presence or absence of cilostazol. In contrast, LPS-induced activation of caspases 9 and 3 were markedly inhibited by cilostazol. Moreover, U0126 and SB203580 effectively blocked the cilostazol-mediated inhibition of this caspase activation (Fig. 7). These results suggest that cilostazol protected HUVECs against LPS-induced apoptosis through inhibiting caspase 9 and 3 activity, and that this was associated with stimulation of ERK 1/2 and p38 MAPK signaling.

Effects on LPS-induced changes in mitochondrial integrity

The results described thus far suggest that activation of the caspase cascade through a mitochondria-dependent mechanism plays a key role in LPS-induced apoptosis and cilostazol-mediated protection. In the next series of experiments, changes in mitochondrial integrity in cells treated with LPS with and without cilostazol and the effects of MAPK inhibitors were examined. Figure 8 shows flow cytometric analyses of DiOC₆(3)-stained cells. In the graphs, the left shift of DiOC₆(3) fluorescence signals indicates depolarization of the mitochondrial membrane potential. LPS significantly depolarized the mitochondrial membrane potential and cilostazol effectively reversed this effect. In the presence of U0126 and SB203580,

cilostazol-mediated prevention of mitochondrial depolarization in LPS-treated cells was abolished (Fig. 8). Consistent with this, cilostazol significantly reduced the LPS-induced release of cytochrome *c* into the cytosol. U0126 and SB203580 also interfered with the action of cilostazol in this process (Fig. 9).

Effects on LPS-induced mitochondrial permeability transition

In the process of mitochondria-dependent apoptosis, disruption of the permeability barrier of the inner mitochondrial membrane (*i.e.*, MPT) precedes the release of cytochrome *c* through the MPT pore [25]. We sought to visualize the LPS-induced MPT by confocal microscopy of cells that were double-stained with the fluorescent dyes TMRM and calcein-AM. Intact mitochondria with a negative membrane potential accumulate the lipophilic cationic dye TMRM. As a result, mitochondrial contours are visualized as bright red spots (left upper and left lower micrographs in Fig. 10A). In cells double-stained with TMRM and mitotracker green (MTG), it is evident that these dyes accumulate at the same loci, as shown in the merged micrograph in the right upper panel of Figure 10A. Calcein, in an acetoxymethylester form (calcein-AM), readily penetrates the cell membrane. In the cytoplasm, esterases hydrolyze calcein-AM into the free acid form. As it is impermeable to the inner mitochondrial membrane, calcein does not enter intact mitochondria, and it resides in the cytoplasm and nuclei (middle and right micrographs in the lower panel of Fig. 10A).

However, *injured* mitochondria in cells exposed to LPS tend to lose TMRM and become permeable to calcein. As a result, it becomes hard to distinguish the mitochondrial contours from the cytosol in micrographs (*e.g.*, the left micrographs in Fig. 10B). These results show evidence of MPT in LPS-treated cells. In this event, as well as mitochondrial depolarization and cytochrome *c* release, as shown in the previous results, cilostazol prevented or delayed LPS-induced MPT, and MEK1/2 inhibitors interfered with this action of cilostazol.

Effects on CREB phosphorylation and Bcl-2 and Bax expression

Phosphorylation of CREB is required for its transcriptional activation [26]. Although PKA is an important kinase for CREB phosphorylation, it has been reported that phosphorylation can occur independently of PKA, through ERK1/2 and p38 MAPK [27]. Thus, we hypothe-

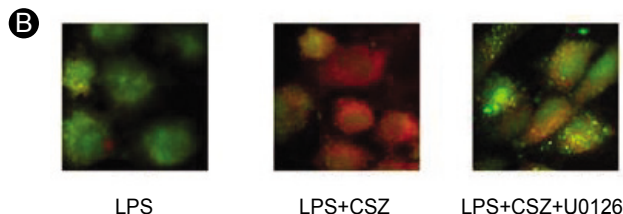
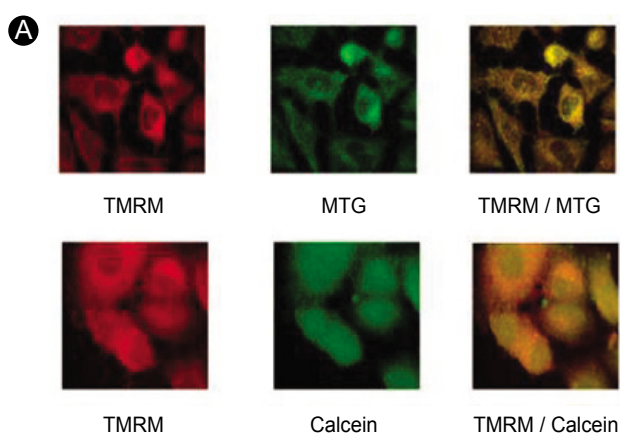


Figure 10. Induction of mitochondrial permeability transition and protection against it by cilostazol, as visualized by confocal micro-scopic. (A) Control cells were double-stained with TMRM/MTG or TMRM/calcein. (B) Cells were treated with 1 µg/mL LPS with and without 10 µM cilostazol in the presence or absence of U0126 (20 µM) for 6 hours and were double-stained with TMRM and calcein-AM.

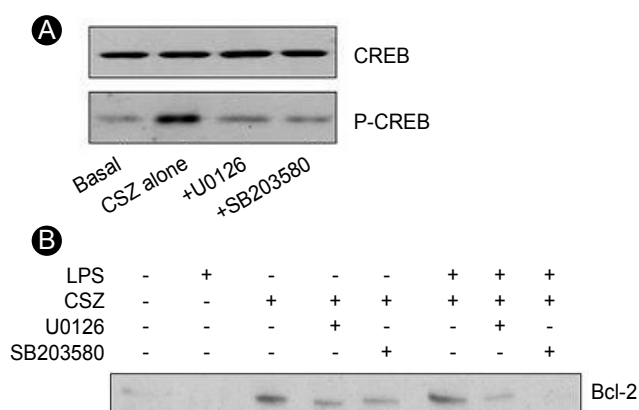


Figure 11. Effects of LPS, cilostazol, and MAPK inhibitors on (A) phosphorylation of CREB, and (B) expression of Bcl-2 and Bax proteins. Cells were treated with 1 µg/mL LPS with and without 10 µM cilostazol in the presence of different MAPK inhibitors (each 20 µM) for 6 hours, and Western blot analysis was performed for phosphorylated CREB, Bcl-2, and Bax proteins in the cell extracts.

sized that cilostazol may stimulate CREB phosphorylation through ERK1/2- and p38 MAPK-dependent pathways. As shown in Figure 11A, MEK1/2 and p38 MAPK inhibitors significantly suppressed the cilostazol-stimulated phosphorylation of CREB. Apoptotic death signals converge on the mitochondria through the activation of pro-apoptotic members of the Bcl-2 family, such as Bax, while Bcl-2 serves as an anti-apoptotic protein [28]. As demonstrated in Figure 11B, cilostazol stimulated Bcl-2, while it suppressed LPS-induced Bax expression. These effects of cilostazol were antagonized by MEK1/2 and p38 MAPK inhibitors.

DISCUSSION

The major findings of the present study are that

cilostazol protected HUVECs against LPS-induced apoptosis by suppressing the mitochondrial permeability transition, the cytosolic release of cytochrome c, and the subsequent activation of caspases. Moreover, it stimulated ERK1/2 and p38 MAPK signaling and increased phosphorylated CREB and Bcl-2 expression, while suppressing Bax expression. In addition, these cilostazol-mediated cellular events could be effectively blocked by MEK1/2 and p38 MAPK inhibitors. The effect of cilostazol in inhibiting LPS-induced apoptosis has been reported previously [10-12]. The present study adds new aspects to the signal transduction pathway of this cilostazol-mediated protection and emphasizes the involvement of the ERK1/2 and p38 MAPK signaling pathways.

LPS, a complex glycoprotein that resides in the outer membranes of Gram-negative bacteria, has been implicated as a causative agent in endothelial injury, a pivotal event that can lead to septic shock and associated syndromes [29]. Previous studies have shown that LPS induces apoptosis in different types of endothelium, including HUVECs [30,31] and lung-derived [32] normal human microvascular endothelial cells. It has also been reported that the release of LPS into the circulation induces endothelial apoptosis *in vivo* and thus causes microvascular injury in numerous tissues, including the lung, gut, and liver, during sepsis [29,33]. Tissues and organs obtained from patients who have died of sepsis and multi-organ failure [29] and animal models of endotoxemia and sepsis reveal enhanced apoptotic cell death [34,35].

Although apoptosis has been implicated as an important mechanism of *in vivo* cell death following LPS exposure, the molecular pathways of apoptosis in endothelial cells are still controversial. Bannerman et al. [30] suggested that LPS-induced apoptosis in HUVECs was mediated through activation of caspase 8 via interaction with Toll-

like receptor (TLR)-4, which is expressed on the endothelial cell membrane. However, Munshi et al. [31] reported that LPS did not exert any significant effect on caspase 8 activity in these cells, and that LPS-induced apoptosis was mediated independently of caspase 8 activation. In the present study, activation of caspase 9 was more prominent than that of caspase 8. Moreover, the caspase 8 inhibitor Z-IETD-FMK was much less effective than the caspase 9 or 3 inhibitors in suppressing LPS-induced apoptosis. This study also demonstrated that deterioration of mitochondrial integrity preceded the execution of apoptosis in LPS-treated cells. These results suggest that the sequential activation of caspases 9 and 3, through a mitochondria-dependent pathway, is a crucial intracellular signaling event in the LPS-induced apoptosis of HUVECs.

MAPKs regulate cellular activities ranging from gene expression, mitosis, motility, and metabolism to apoptosis. It is generally believed that ERKs are important for cell survival, while JNKs and p38 MAPKs have been deemed stress-responsive, and thus involved in apoptosis. However, the regulation of apoptosis by MAPKs is more complex than once thought and remains controversial. The ERK1/2 pathway is primarily induced in response to mitogens and growth factors and plays a major role in regulating cell growth, survival, and differentiation [36,37]. In contrast, the JNK and p38 pathways are activated in response to chemical and environmental stresses. Their activation is frequently associated with the induction of apoptosis [15,37].

The present study suggests that the activation of ERK1/2 and p38 MAPK plays an important role in the cilostazol-mediated inhibition of LPS-induced apoptosis. The drug induced sustained elevation of phosphorylated ERK1/2 and p38. Moreover, the ERK1/2 upstream kinase MEK1/2 inhibitor U0126 [18] and the p38 MAPK inhibitor 203580 markedly suppressed the cilostazol-mediated inhibition of LPS-induced apoptosis and activation of caspases 9 and 3. The effects of the MAPK inhibitors on the mitochondrial events associated with cilostazol-mediated protection were consistent with the belief that these MAPKs play pivotal roles in the cellular signaling events for the cilostazol-mediated *anti*-apoptotic effect. Furthermore, confocal microscopy provided direct evidence for a role of these MAPKs in the cilostazol-mediated prevention of the mitochondrial permeability transition, a key event for the initiation of mitochondria-dependent apoptotic signaling.

It is generally accepted that cAMP-mediated trans-

criptional responses involve the ability of PKA to phosphorylate CREB [26]. However, an alternative mechanism has been proposed whereby cAMP promotes phosphorylation of CREB through ERK1/2 and p38 MAPK, and perhaps other protein kinases too. In the present study, cilostazol-stimulated phosphorylation of CREB was significantly reduced by MEK1/2 and p38 MAPK inhibitors, indicating the involvement of these MAPKs in the signaling of CREB phosphorylation. The cyclic AMP response element is a major positive regulatory site in the Bcl-2 promoter [38]. Thus, the increased expression of Bcl-2 by cilostazol and its inhibition by MAPK inhibitors in this study seem to reflect the consequences of CREB phosphorylation.

In conclusion, the present study demonstrated that cilostazol protected HUVECs against LPS-induced apoptosis by suppressing mitochondria-dependent apoptotic signaling. Activation of ERK1/2 and p38 MAPKs, and subsequent stimulation of CREB phosphorylation and Bcl-2 expression, may be responsible for the cellular signaling mechanism of cilostazol-mediated protection.

REFERENCES

1. Kimura Y, Tani T, Kanbe T, Watanabe K. Effect of cilostazol on platelet aggregation and experimental thrombosis. *Arzneimittelforschung* 1985;35:1144-1149.
2. Kohda N, Tani T, Nakayama S, et al. Effect of cilostazol, a phosphodiesterase III inhibitor, on experimental thrombosis in the porcine carotid artery. *Thromb Res* 1999;96:261-268.
3. Tanaka K, Gotoh F, Fukuuchi Y, et al. Effects of a selective inhibitor of cyclic AMP phosphodiesterase on the pial microcirculation in feline cerebral ischemia. *Stroke* 1989;20:668-673.
4. Dawson DL, Cutler BS, Meissner MH, Strandness DE Jr. Cilostazol has beneficial effects in treatment of intermittent claudication: results from a multicenter, randomized, prospective, double-blind trial. *Circulation* 1998;98:678-686.
5. Lefer AM, Lefer DJ. Pharmacology of the endothelium in ischemia-reperfusion and circulatory shock. *Annu Rev Pharmacol Toxicol* 1993;33:71-90.
6. Ten VS, Pinsky DJ. Endothelial response to hypoxia: physiologic adaptation and pathologic dysfunction. *Curr Opin Crit Care* 2002;8:242-250.
7. Minor T, Isselhard W. Role of the hepatovasculature in free radical mediated reperfusion damage of the liver. *Eur Surg Res* 1993;25:287-293.
8. Scalia R, Pearlman S, Campbell B, Lefer AM. Time course of endothelial dysfunction and neutrophil adherence and infiltration during murine traumatic shock. *Shock* 1996;6:177-182.

9. Hack CE, Zeerleder S. The endothelium in sepsis: source of and a target for inflammation. *Crit Care Med* 2001;29(7 Suppl):S21-S27.
10. Kim KY, Shin HK, Choi JM, Hong KW. Inhibition of LPS-induced apoptosis by cilostazol in human umbilical vein endothelial cells. *J Pharmacol Exp Ther* 2002;300:709-715.
11. Hong KW, Kim KY, Shin HK, et al. Cilostazol prevents tumor necrosis factor- α -induced cell death by suppression of phosphatase and tensin homolog deleted from chromosome 10 phosphorylation and activation of Akt/cyclic AMP response element-binding protein phosphorylation. *J Pharmacol Exp Ther* 2003;306:1182-1190.
12. Choi JM, Shin HK, Kim KY, Lee JH, Hong KW. Neuroprotective effect of cilostazol against focal cerebral ischemia via antiapoptotic action in rats. *J Pharmacol Exp Ther* 2002;300:787-793.
13. Johnson GL, Lapadat R. Mitogen-activated protein kinase pathways mediated by ERK, JNK, and p38 protein kinases. *Science* 2002;298:1911-1912.
14. Wada T, Penninger JM. Mitogen-activated protein kinases in apoptosis regulation. *Oncogene* 2004;23:2838-2849.
15. Davis RJ. Signal transduction by the JNK group of MAP kinases. *Cell* 2000;103:239-252.
16. Pastorino JG, Chen ST, Tafani M, Snyder JW, Farber JL. The overexpression of Bax produces cell death upon induction of the mitochondrial permeability transition. *J Biol Chem* 1998;273:7770-7775.
17. Lemasters JJ, Nieminen AL, Qian T, et al. The mitochondrial permeability transition in cell death: a common mechanism in necrosis, apoptosis and autophagy. *Biochim Biophys Acta* 1998;1366:177-196.
18. Favata MF, Horiuchi KY, Manos EJ, et al. Identification of a novel inhibitor of mitogen-activated protein kinase kinase. *J Biol Chem* 1998;273:18623-18632.
19. Cirillo PF, Pargellis C, Regan J. The non-diaryl heterocycle classes of p38 MAP kinase inhibitors. *Curr Top Med Chem* 2002;2:1021-1035.
20. Bennett BL, Sasaki DT, Murray BW, et al. SP600125, an anthranyrazolone inhibitor of Jun N-terminal kinase. *Proc Natl Acad Sci U S A* 2001;98:13681-13686.
21. Ozoren N, Kim K, Burns TF, Dicker DT, Moscioni AD, El-Deiry WS. The caspase 9 inhibitor Z-LEHD-FMK protects human liver cells while permitting death of cancer cells exposed to tumor necrosis factor-related apoptosis-inducing ligand. *Cancer Res* 2000;60:6259-6265.
22. Akita K, Ohtsuki T, Nukada Y, et al. Involvement of caspase-1 and caspase-3 in the production and processing of mature human interleukin 18 in monocytic THP1 cells. *J Biol Chem* 1997;272:26595-26603.
23. van Noorden CJ. The history of Z-VAD-FMK, a tool for understanding the significance of caspase inhibition. *Acta Histochem* 2001;103:241-251.
24. Talanian RV, Quinlan C, Trautz S, et al. Substrate specificities of caspase family proteases. *J Biol Chem* 1997;272:9677-9682.
25. Kroemer G, Dallaporta B, Resche-Rigon M. The mitochondrial death/life regulator in apoptosis and necrosis. *Annu Rev Physiol* 1998;60:619-642.
26. Mayr B, Montminy M. Transcriptional regulation by the phosphorylation-dependent factor CREB. *Nat Rev Mol Cell Biol* 2001;2:599-609.
27. Nishihara H, Hwang M, Kizaka-Kondoh S, Eckmann L, Insel PA. Cyclic AMP promotes cAMP-responsive element-binding protein-dependent induction of cellular inhibitor of apoptosis protein-2 and suppresses apoptosis of colon cancer cells through ERK1/2 and p38 MAPK. *J Biol Chem* 2004;279:26176-26183.
28. Sprick MR, Walczak H. The interplay between the Bcl-2 family and death receptor-mediated apoptosis. *Biochim Biophys Acta* 2004;644:125-132.
29. Hotchkiss RS, Swanson PE, Freeman BD, et al. Apoptotic cell death in patients with sepsis, shock, and multiple organ dysfunction. *Crit Care Med* 1999;27:1230-1251.
30. Bannerman DD, Tupper JC, Ricketts WA, Bennett CF, Winn RK, Harlan JM. A constitutive cytoprotective pathway protects endothelial cells from lipopolysaccharide-induced apoptosis. *J Biol Chem* 2001;276:14924-14932.
31. Munshi N, Fernandis AZ, Cherla RP, Park IW, Ganju RK. Lipopolysaccharide-induced apoptosis of endothelial cells and its inhibition by vascular endothelial growth factor. *J Immunol* 2002;168:5860-5866.
32. Hoyt DG, Mannix RJ, Gerritsen ME, Watkins SC, Lazo JS, Pitt BR. Integrins inhibit LPS-induced DNA strand breakage in cultured lung endothelial cells. *Am J Physiol* 1996;270:L689-L694.
33. Wort SJ, Evans TW. The role of the endothelium in modulating vascular control in sepsis and related conditions. *Br Med Bull* 1999;55:30-48.
34. Haimovitz-Friedman A, Cordon-Cardo C, Bayoumy S, et al. Lipopolysaccharide induces disseminated endothelial apoptosis requiring ceramide generation. *J Exp Med* 1997;186:1831-1841.
35. Zhang XM, Morikawa A, Takahashi K, et al. Localization of apoptosis (programmed cell death) in mice by administration of lipopolysaccharide. *Microbiol Immunol* 1994;38:669-671.
36. Cobb MH. MAP kinase pathways. *Prog Biophys Mol Biol* 1999;71:479-500.
37. Xia Z, Dickens M, Raingeaud J, Davis RJ, Greenberg ME. Opposing effects of ERK and JNK-p38 MAP kinases on apoptosis. *Science* 1995;270:1326-1331.
38. Xiang H, Wang J, Boxer LM. Role of the cyclic AMP response element in the Bcl-2 Promoter in the regulation of endogenous Bcl-2 expression and apoptosis in murine B Cells. *Mol Cell Biol* 2006;26:8599-8606.